Masonry Texture Reconstruction through High Frequency 3D GPR Survey for Building Seismic Assessment

Federico Lombardi (*), Maurizio Lualdi and Elsa Garavaglia

Department of Civil and Environmental Engineering, Politecnico di Milano, Piazza Leonardo da Vinci 32, 20133 Milan, Italy

* Corresponding author. Tel.: +390223994226. email: federico.lombardi@polimi.it

Abstract

The geometrical texture and morphology of a masonry wall section represent a key parameter when evaluating its seismic response. Such estimate is commonly performed through localised, semi-destructive methods, regarding which Ground Penetrating Radar (GPR) could emerge as an effective alternative survey method, due to its high-resolution, scalable and non-destructive approach. This research has targeted the reconstruction of the geometrical properties of a heterogeneous masonry section through a high-frequency, 3D GPR investigation to evaluate the retrievable information, and the achieved results demonstrated the operational potential of the technique in providing earlier qualitative and quantitative information on the structure seismic behaviour.

Keywords: Ground Penetrating Radar; Seismic assessment; Masonry texture reconstruction; Signal processing; NDT surveys.

1 . INTRODUCTION

The definition and characterisation of the texture of a masonry wall represent priority topics not only for building evaluation and diagnosis, but also within the seismic assessment and hazard mitigation domain, as the wall capability of sustaining horizontal in-plane and out–of–plane actions can be estimated provided that the typology, stratigraphy and internal construction and condition of the masonry structure are accurately determined. With all the mentioned attributes available, it is in principle possible to calculate the strength of the investigated masonry as a function of that of the components [1], [2].

Such relevance is enhanced by the fact that earthquake aftermaths are increasingly demonstrating the inefficacies of commonly found masonry textures in preventing the activation of collapsing mechanisms.

Even if structural flaws can be principally attributed to improper construction techniques of civil structures in high seismic risk zones, they are also a direct consequence of the lack of preventive maintenance, as well as enlargement interventions or structural modifications performed without an adequate historical knowledge of the building.

It is therefore straightforward that many difficulties could be eliminated if better technical information regarding the mechanical characteristics of historic masonry are available. To achieve this scope, it is in principle essential to gather as much information as possible to understand how the structure under investigation has evolved over time, the modifications, replacements or adjustments that might have taken place and the correspondent time period, as these details can guide in formulating assumptions on the original construction approach, essential information for estimating the seismic response of the construction. In particular, a high percentage of voids in masonry panels and lack of effective connections among structural components, as well as low-quality stone units and mortar used in the building process, can lead to a degraded seismic resistance. It is therefore straightforward that such constituent materials heterogeneity together with the great variability of the possible construction techniques have made it difficult to develop reliable modelling schemes, in particular for masonry structures. As a consequence, the described information is typically available after the occurrence of a seismic events, which means that the seismic assessment of the structure is assessed retrospectively, starting from the damage sustained [3], [4], [5], [6], [7]. Although over the years such methodological approach has resulted in the development of highly accurate assessment reports [8] that allow to precisely correlate each single structural topology to a specific statistical vulnerability index and related seismic hazard curves [9][10][11], it would be important, instead, to evaluate the status and vulnerability of a masonry given the intact building, so that targeted interventions can be planned and put forward [12].

It is therefore obvious that in order to qualify the state of preservation of stone or brick masonry walls, a knowledge of the inside is essential. The analysis of these structural features is often carried out by locally detaching and removing the plaster wall cover to highlight the masonry behind. Given the invasive nature of such investigation methodologies, a limited number of samples, typically located in secondary areas of the building, are extracted, hence limiting the thoroughness of the assessment and the confidence in claiming that the highlighted local behaviour effectively reflects the building as a whole one.

An operational breakthrough within these investigations can be achieved using Ground Penetrating Radar methodology [13], [14], thanks to its non-destructive principles and high resolution performance, which might allow the survey of multiple areas without the need for uncovering the masonry and consequently the investigation of extended portions that could lead to a more reliable and accurate assessment [15], [16], [17], [18], [19]. GPR technique utilises high frequency electromagnetic waves reflections at boundaries between materials exhibiting different electrical properties to determine the structure of the investigated area, which in the context of structures and buildings, typically includes voids, areas of wet material, and reinforcement structural element [20], [21], [22], [23]. Within these scopes, GPR has proven to be a highly effective and successful techniques, as reported in several reports and case studies [24], [25], [26], [27], [28].

The estimation of the mechanical properties of a masonry wall can be obtained by considering the behaviour of an ideal masonry wall and the mechanical properties of the constituent materials (stones, bricks, mortars, etc.), described by the following parameters [1], [29] [30]:

- Conservation state of bricks and mortar, in particular possible weathering effects and material erosion.
- Stone/brick dimension properties, with respect to the longer axis of each single element.
- Stone/brick shape, in particular concerning the associable morphology of the element (from pebbles to perfectly cut stones) for each masonry leaf.
- Wall leaf connections, factors related to the presence of headers that might connect adjacent leaves.
- Horizontal bed joints characteristics, in particular their continuity.
- Vertical bed joint characteristics, in particular their staggering pattern.

By assigning a qualitative index to each of these factors, typically based on a fulfilled – not fulfilled scale, it is possible to calculate a numerical value representing the behaviour of the masonry that is correlated to its mechanical parameters (compressive strength, shear strength and modulus of elasticity). Despite being not completely exhaustive, such strategy has demonstrated its efficacy in providing a general overview of the masonry status which might help and assist the execution of experimental measurements targeting the materials mechanical properties.

Although it is a promising subject, few GPR studies have targeted the masonry texture definition under this operational perspective, revealing the difficulty inherent to this complex scenario [31], [32], [33].

The deployment of GPR as a tool for the diagnosis of a structure, being this in terms of maintenance, restoration or safety assessments, requires to accurately evaluate the internal construction and condition of masonry, its geometrical morphology and composition, as well as the capability of determining the possible coexistence of modern constructive elements with ancient masonry ones. The challenge is therefore to precisely reconstruct the order and the alternation between bricks, determine their size and orientation, and delineate the mortar joints distribution, all tasks that requires a high resolution definition of shallow objects with limited size and potentially limited electromagnetic impedance contrast. Finally, it must be considered that such assessment should be performed without excessively altering or damaging the surface, and potentially from one side only.

These requirements necessarily imply the deployment of a survey platform optimised for the task, as it should answer two main operational demands. First of all, the need for sufficient resolution to detect and image elements within the first 2-5 centimetres, as well as to produce results as much informative and readable as possible [34], [35], [36], [37]. This aspect is also a consequence of the well-known GPR effectiveness dependency on the user ability to interpret the obtained images. Secondly, the necessity of moving towards a three dimensional acquisition approach, due to the shallow depth of the targets of interest, their limited size and the level of detail required for the subsurface characterisation [38], [39]. All these aspects prevent the adoption of a sparse 2D profile approach, resulting in the necessity of collecting a 3D data volume spatially compliant with the Nyquist spatial sampling criterion, in order to avoid aliasing during data reconstruction [40].

Under this perspective, the aim of the following research is to determine the potential of GPR methodologies in providing useful, i.e. quantitative and numerical, details related to the geometrical morphology of a masonry wall, to a level such that the extracted information can be effectively employed for determining the quality level of the masonry and to support the building assessment procedures, essential precondition for bringing the GPR technique into practice for on-site investigations. For this reason, a portion of a wall with known masonry architecture was surveyed with a high frequency GPR platform, making it possible to assess the reliability of the methodology with respect to the previously highlighted parameters.

The paper is organised as follows. Section 2 describes the carried out geophysical survey methodology and the survey strategy, while in Section 3 the obtained GPR results and the analysis of the reconstruction performance are presented and discussed. Finally, Section 5 integrates the obtained reconstruction in the evaluation of the masonry quality, and a summary of the findings and potential developments are briefly addressed in Section 6.

. SURVEY AREA AND METHODOLOGY

For the purpose of the study, a recently covered wall has been selected to evaluate the GPR potential in reconstructing the morphology of masonry buildings. The site has been chosen as it presents several critical aspects in terms of masonry design, constituent elements distribution, size and geometry, as can be seen in Fig 1.

Figure 1: Experimental area.

From the photographs prior to the restructuring, it can be seen that the selected site is composed of three main areas: a first sector exhibiting a geometrically regular brickwork (marked A in Fig. 1) on top of a segmental arch (marked B in Fig. 1), i.e. an arch whose intrados is circular but less than a semicircle, a sign of a former aperture within the masonry wall, visible with its correspondent jack arch in the lower part of Fig. 1 (marked

C in Fig. 1). This represents the typical relieving arch design, built over a lintel or a jack arch to divert loads and hence relieving the lower member from excessive loading.

An area of 70-by100 cm has been surveyed (Fig. 2a), covering the first two previously described areas, as shown in Fig. 2b.

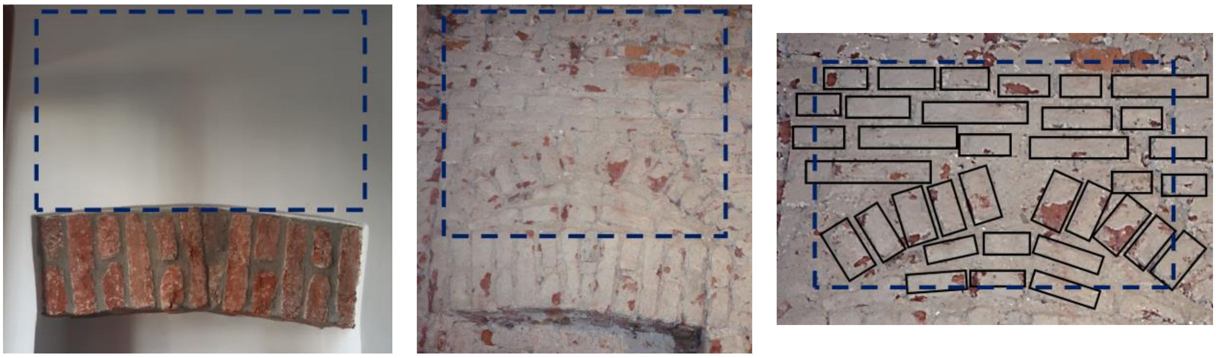

Figure 2: survey area details.

Within these (Fig. 2c), the portion of the upper area that has been acquired consists of 3 rows of bricks each of them including 5 to 6 elements, unevenly distributed, as well as inhomogeneous mortar joint thickness, while the underlying segmented arch includes 9 voussoirs (an additional element straddles the acquisition boundaries) with a maximum skewback angle of 35 degrees with respect to the arch keystone, and a core of brickwork between the underside of the arch and the top of the lintel.

GPR data were acquired using an IDS Georadar TR-SHF radar, a ground coupled impulse system with a central frequency and a bandwidth of 3 GHz. The device carries two bow-tie antennas spaced 6 cm and oriented perpendicular to the survey line (Fig. 3a). The sensor head, which is essentially a passive component weighting approximately 2 kg and with a size of 6 by 12 cm, is connected to a central unit responsible for the generation, transmission and reception of the signal. The required dense and regular 3D acquisition grid has been obtained by directly placing a cardboard variant of the PSG (Pad System for Georadar, [41]) over the wall (Fig. 3b), ensuring parallelism between adjacent profiles, while the inline sampling was controlled through an odometric wheel directly connected to the sensor head.

(a) (b)

Figure 3: (a) employed GPR platform and (b) survey geometry.

In this case, data were acquired along the ceilings to the floor direction. However, as logistic constraints might necessitate different acquisition geometries compared to the chosen one, two orthogonal volumes have been acquired to assess eventual differences in the imaging results. The choice of the orthogonal direction derived from the fact that, despite not expected to exhibit a strong polarimetric response, the regular geometry of a brickwork, particularly the vertical and horizontal mortar joints, might impact the magnitude of the scattering response [42]. Moreover, in case of structural metallic reinforcement elements such scheme will ensure a full detection, as a consequence of the well-known sensitivity to polarisation of highly conductive linear targets [43]. Precise correspondence among the acquired samples has been ensured by rotating the system with respect to the reflection centre of the antennas, while maintaining the same acquisition geometry.

Acquisition parameters are provided in Table I. For each volume, a total of 150 profiles have been acquired, with an acquisition time of approximately 60 minutes.

Table I: acquisition parameters.

Parameter	**Value**
Inline sampling	0.4 cm
Crossline sampling	0.7 cm
Time sampling	0.039 ns
Time window	20 ns
Antenna separation	6 cm
Antenna height	< 1 cm
Antenna frequency	3 GHz

System bandwidth	3 GHz

Considering the resolution performance and consequently the capability of correctly recognising the bricks layer, as a general rule two events can be distinguished if the targets are separated in time by a time difference at least equal to half of the envelope width. The emitted waveform of the employed GPR system exhibits a -3 dB envelope width of approximately 0.14 ns, resulting in a required time difference between the top and the bottom of each layer of 0.14 ns in order to be separated. Considering that the dielectric constant of typical plaster used in masonry lies within the 3-5 range, even considering a velocity of 17 cm/ns, i.e. the less favourable conditions, the spectral characteristics of the system allows for a proper separation between the plaster layer, which has a thickness of 3 cm, and the upper faces of the brickwork, as the temporal extension of the plaster covering is approximately 0.17 ns.

As mentioned in the previous section, although in some cases it might be easier to detect subsurface features from raw GPR data, migration represents one of the most useful tool to facilitate a correct interpretation and geometrical reconstruction of the subsurface features. Therefore, the results of the experimentation are presented both in term of raw time slice, obtained by applying a time calibration and a linear frequency filtering to remove out of band noise, and a set of depth slices, retrieved via Kirchhoff migration. Details on the processing algorithms are provided in Table II.

Table II: data processing details.

Processing step	**Description**
Time calibration	Time shift.
Trace alignment	Correlation window.
Frequency filtering	Zero-phase Butterworth filter. Frequency range 1 – 4 GHz.
Velocity analysis	Hyperbola fitting. Mean aperture: 5 cm.
3D migration	2D-2step approach.

As a result of the velocity analysis, providing a velocity of approximately 15 cm/ns, the vertical resolution limit can be set at approximately 1.25 cm considering the central frequency of 3 GHz, once again demonstrating the background separation ability.

2 . GPR RESULTS

The following section presents the obtained GPR results, for both raw/processed data and horizontal/vertical antenna orientation. To quantitatively assess the detection accuracy and reconstruction performance, the following aspects have been evaluated: for the raw data, the detection performance, defined as the comparison between the number of identifiable elements within the time slice ensemble and the actual one. In addition to this, the migrated data have been assessed also considering the reconstruction accuracy, determined as the evaluation of the estimated element size and the actual one. Such decision has been taken considering that the resolution along the crossline direction in unfocussed data depicts low resolution features owing to the long tails of the diffraction hyperbola, hence the factual size and location of the scattering element is typically erroneous.

2.1 Unmigrated time slices

Unmigrated time slices produced by the horizontal configuration, i.e. with the dipoles perpendicular to the survey direction, are presented in Fig 5.

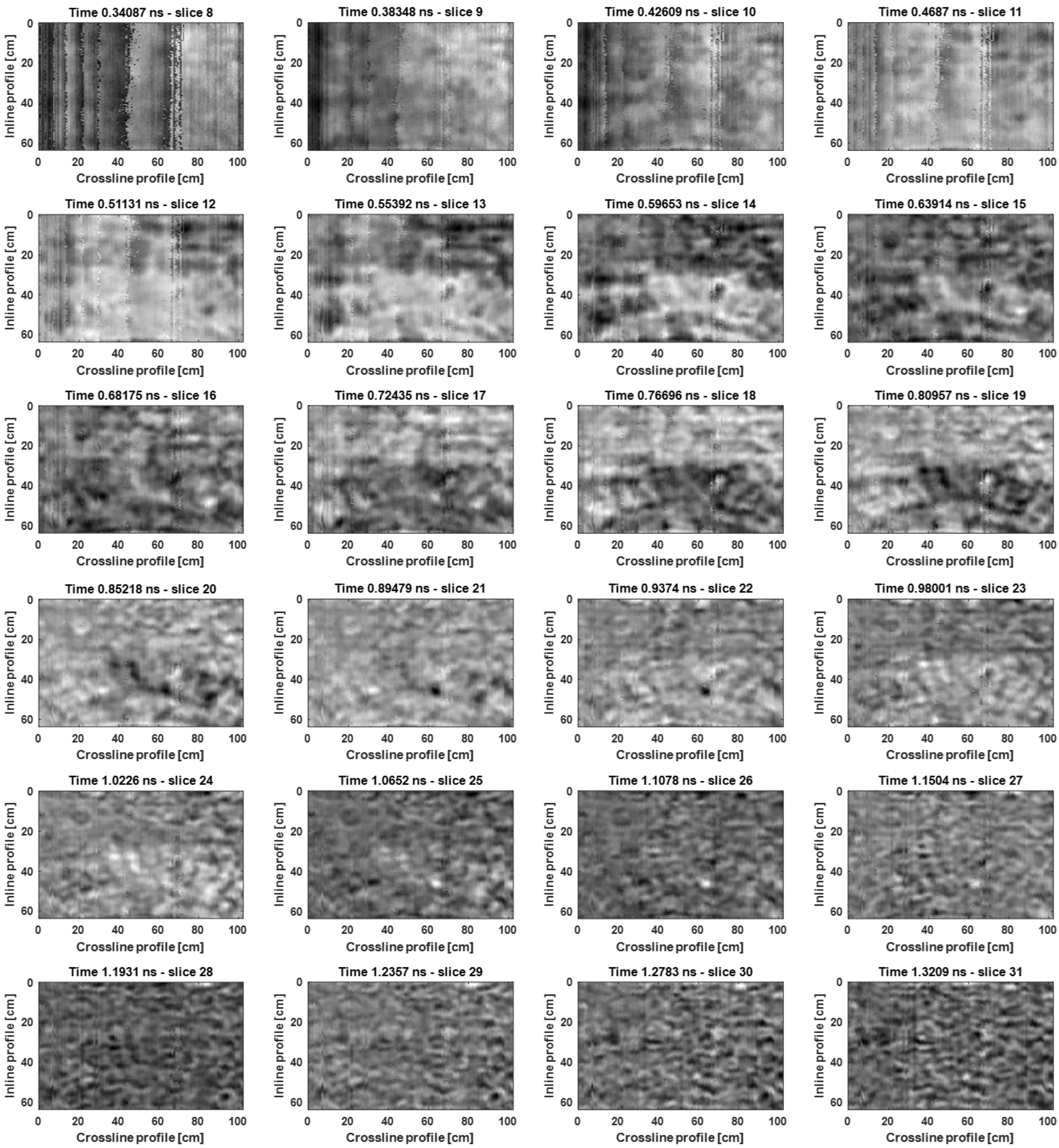

Figure 5: GPR results, unmigrated horizontally oriented time slices.

From the analysis of the slices ensemble, the two different morphologies previously highlighted can be identified. In particular, the intrados and the extrados of the segmented arch are evident (particularly from slice 13 to slice 20 of Fig. 5) in the lower part of the slice (inline direction interval from 30 cm onward), spanning the entire crossline dimension, while the geometrically regular brickwork can be delineated within the area above. The scattering contribution from the masonry can be assumed to start from the eleventh slice after the background reflection, corresponding to a time interval of 0.46 ns and resulting in an estimated plaster thickness of approximately 3.5 cm, which is closely resembling the existent value. Both the areas exhibit a similar temporal extension, lasting for roughly 20 slices and consequently resulting in an estimated layer thickness of 0.8 ns, which leads to a thickness of 12 cm. Finally, mortar joints can be easily delineated, and in particular the horizontal bed ones, as a consequence of the orientation of the antenna pattern, which can better image the horizontal mortar lines compared to the vertical ones.

It is therefore possible to extract some quantitative information on the geometrical composition of the masonry, even if it is clear that the actual number of bricks would be difficult to determine. This remark applies to the relieving arch as well, for which the contour can be accurately delineated, but several uncertainties remain when attempting to enumerate each voussoir. Carefully analysing the set slice by slice, it is possible to determine a quantitative indication of the level of fidelity that can be obtained under the perspective of defining the geometrical texture of the wall. In particular, in each slice the potential presence of a masonry element has been highlighted to obtain the final texture map provided in Fig. 6, along with the actual status.

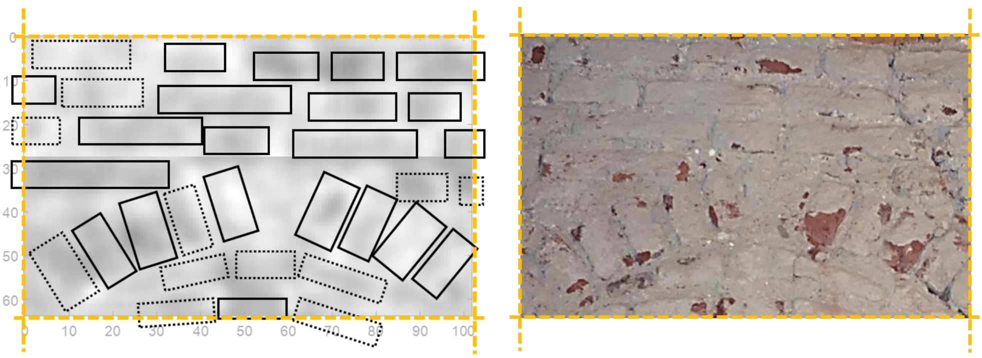

Figure 6: Reconstruction performance, unmigrated horizontally oriented time slices.

The achieved detection capability, generated by approximately 8 to 10 slices and relying to a certain extent on the user interpretation ability, is numerically described in Table 3.

Table III: Numerical reconstruction performance, unmigrated horizontally oriented time slices.

	Investigated area	Investigated sector	Estimated number of elements	Actual number of elements
	Upper area	First row	4	5

		Second row	4	5
		Third row	4	5
	Lower area	Relieving arch	7	9
		Brickwork core	2	9

To assess the effects of a change in the survey direction, the same set of slices is presented for the orthogonally oriented acquisition, i.e. vertical configuration (Fig. 7).

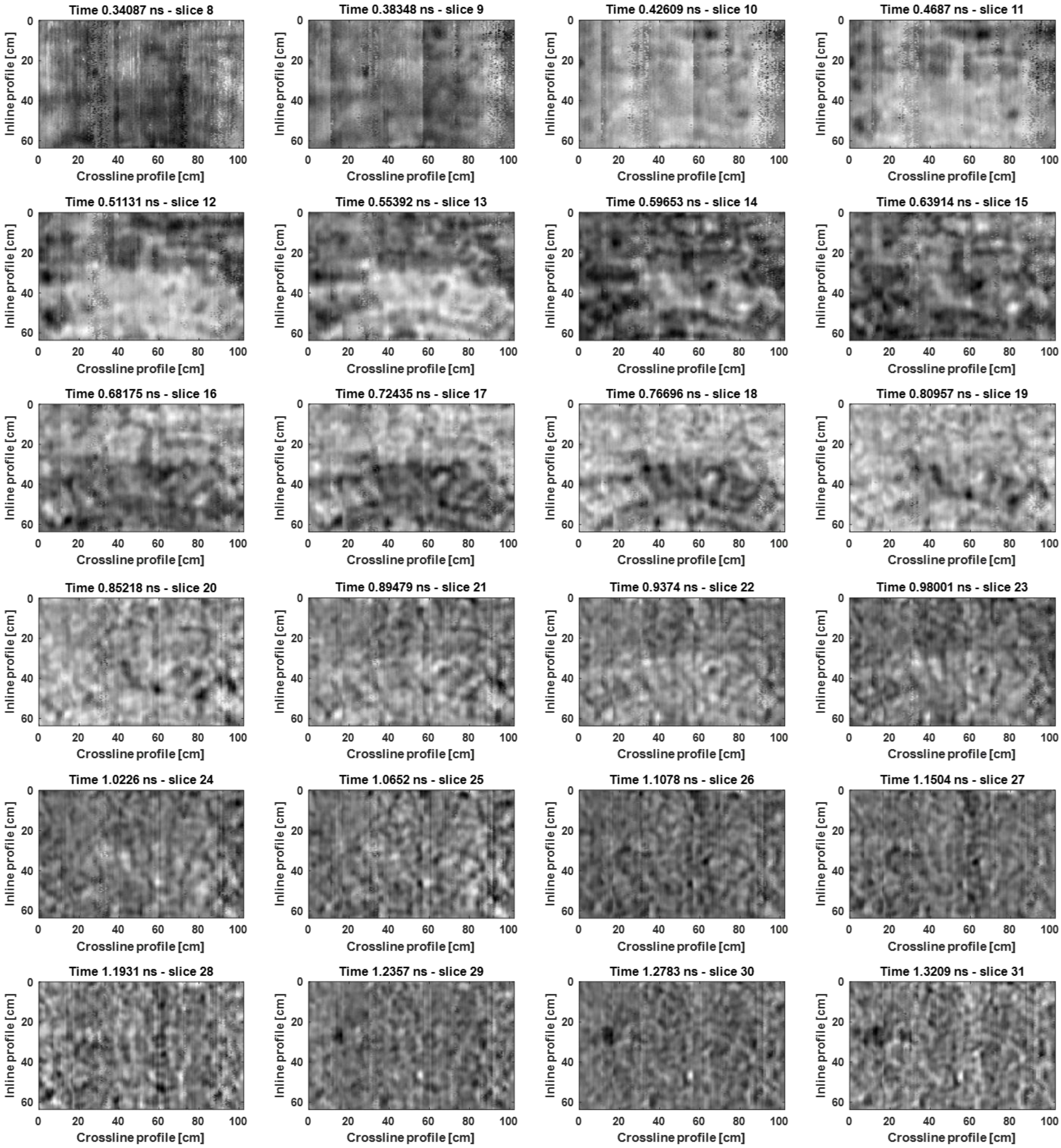

Figure 7: GPR results, unmigrated vertically oriented time slices.

As a first strand of the analysis, it can be seen that, compared to Fig.6, there are no noticeable differences in the imaging performance, as also changing the survey direction still manages to highlight the two masonry areas previously described. A comparable similarity exists also with respect to the amplitudes distribution of the two ensembles, both presented with the same dynamic range for a proper comparison.

However, from a deeper analysis, it emerges that the vertical mortar joints are better imaged, as expected from the previous considerations on the antenna pattern geometry, and consequently the reconstruction of the elements exhibiting a limited height turns out to be facilitated, as shown in Fig. 8 and numerically described in Table IV.

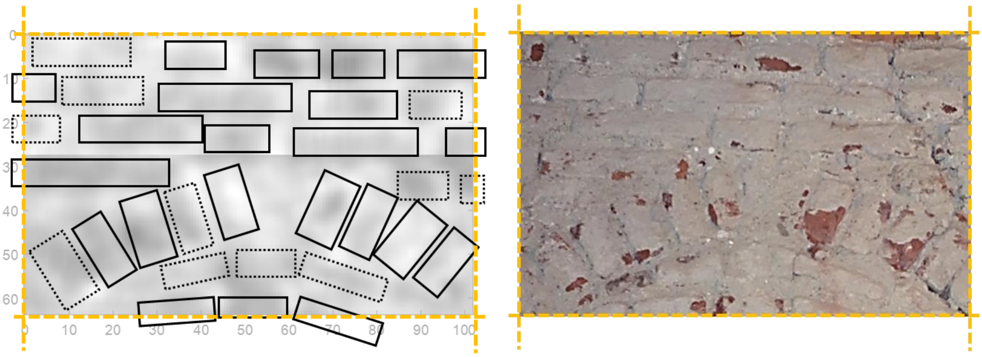

Figure 8: Reconstruction performance, unmigrated vertically oriented time slices.

Table IV: Numerical reconstruction performance, unmigrated vertically oriented time slices.

	Investigated area	**Investigated sector**	**Estimated number of elements**	**Actual number of elements**
	Upper area	First row	4	5
		Second row	3	5
		Third row	4	5
	Lower area	Relieving arch	7	9
		Brickwork core	4	9

What can be achieved, in this case through the interpretation of a slightly lower number of slices (6 to 8 approximately) is still a partial reconstruction, as the advantages in determining the vertical discontinuities is balanced by the limited readability of the image. Concerning the segmented arch, no significant discrepancies exist with the orthogonal correspondent, in terms of both imaging readability and level of information that gathers. The comparison between the two schemes demonstrates that, although some differences can be appreciated, no significant advantages exist in choosing a specific acquisition direction, meaning that such aspect does not represent a critical parameter when planning the survey.

Summarising what can be extract from the presented results, it can be concluded that unmigrated data, although providing acceptable and satisfactory results, allows mostly for a qualitative interpretation, as only the appearance of the investigated area can be characterised and retrieved, but a complete reconstruction is still out of reach. While missing the elements close to the boundaries of the acquisition pad represents a solvable issue when approaching the survey on a larger scale, several bricks are not detectable regardless their size or geometry.

2.2 Migrated depth slices

To solve the challenge of quantitatively reconstruct the masonry wall, i.e. determine the number and actual location of each element, migrated data are presented for each acquisition scheme, starting from the horizontally oriented volume (Fig. 9). As described in Table II, a limited aperture value has been selected to further improve the resolution of the produced images and to avoid the introduction of processing artefacts.

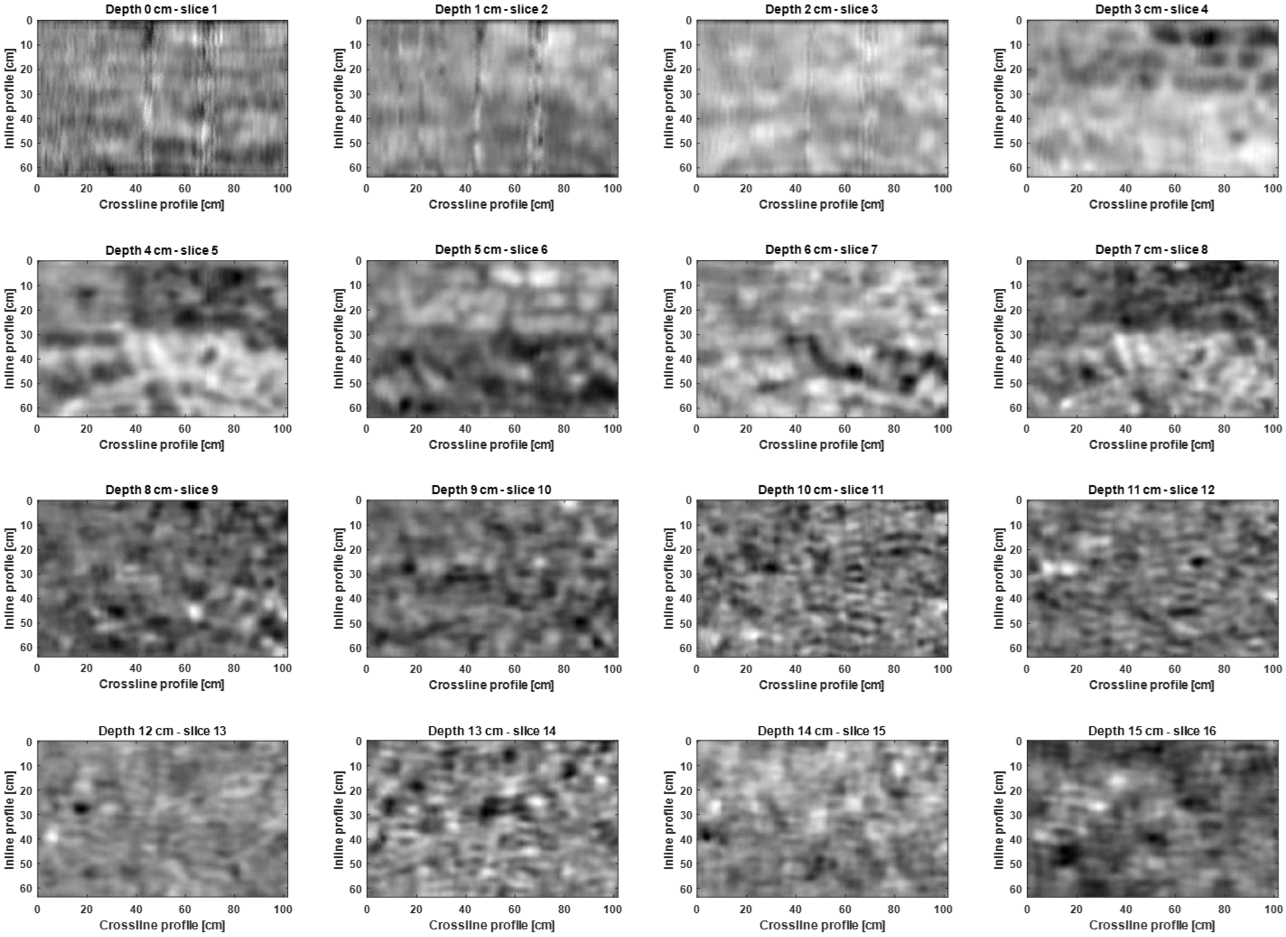

Figure 9: GPR results, migrated horizontally oriented depth slices.

As expected, the additional processing step has the benefit of accurately reconstructing each scattering element and the relative boundaries, at the same time sharpening the image, as can be clearly seen in the depth slices ensemble. In agreement with the predicted plaster thickness and brick thickness, masonry layer appears at a depth of 3 cm, and its scattering contributions vanishes with depths greater than 11 cm. What can be also noticed is that the signature of the arch appears slightly deeper, meaning either a locally increased covering thickness or an underestimated velocity value. The close correspondence with the existent masonry texture is particularly evident for the geometrically regular brickwork (slice 4 in Fig. 9).

The additional advantage of analysing migrated data over unmigrated ones is that it requires a significantly reduced number of radar slices to properly reconstruct the masonry morphology, 2 to 3 images, thus mitigating as well the effects of the user familiarity in interpreting the data. Detection performance are sketched in Fig. 10.

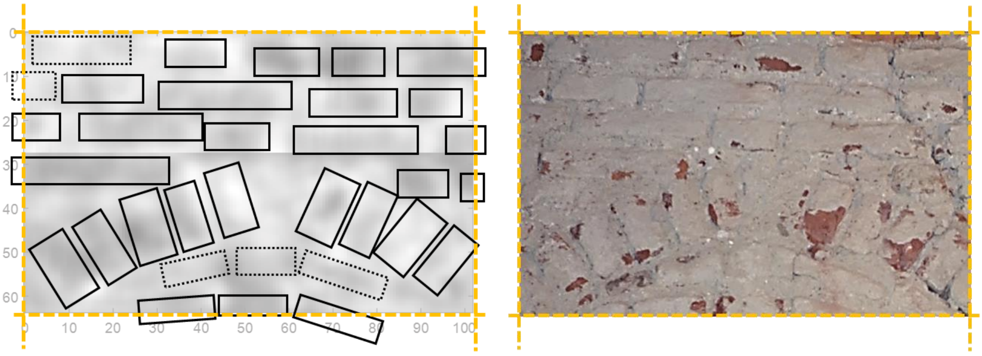

Figure 10: Reconstruction performance, migrated horizontally oriented depth slices.

As before, Table V describes the quantitative results in terms of detected masonry elements with respect to the existent ones.

Table V: Numerical reconstruction performance, migrated horizontally oriented depth slices.

	Investigated area	**Investigated sector**	**Estimated number of elements**	**Actual number of elements**
	Upper area	First row	4	5
		Second row	4	5
		Third row	5	5
	Lower area	Relieving arch	9	9
		Brickwork core	6	9

The texture is clearly identifiable, and the actual number of elements and their size can be guessed, with a remarkable level of accuracy and detail. Only the smallest and less regularly organised elements still represent a challenge, even if their presence can be supposed considering the texture of the surrounding neighbourhood. As a figure of merit, Table VI describes the obtained accuracy in determining the size of brick examples compared to the actual values.

Table VI: Numerical reconstruction accuracy, migrated horizontally oriented depth slices.

Brick example	Element label	Estimated size	Actual size
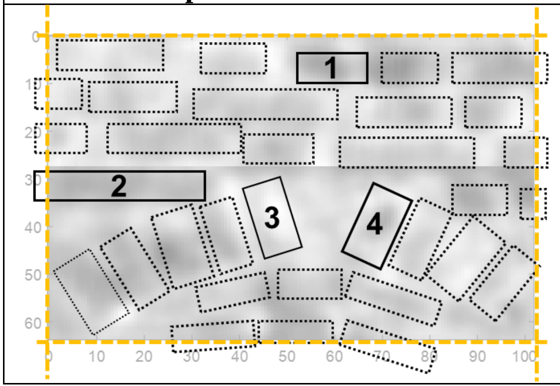	1	Height: 7.5 cm Length: 14 cm	Height: 6.5 cm Length: 14 cm
	2	Height: 6 cm Length: 30 cm	Height: 5 cm Length: 27 cm
	3	Height: 12 cm Length: 7 cm	Height: 12 cm Length: 6 cm
	4	Height: 13 cm Length: 7 cm	Height: 12 cm Length: 6.5 cm

Given the spatial uncertainty given by the system resolution, it is evident the close match between the retrieved data and the factual one, even for bricks with limited size, as for the case of element labelled 1 in Table VI.

From the results, it is evident that a number of parameters and features that can be used for evaluating the quality of the masonry can be extracted, including the disposition of the vertical joints, their offset to the normal direction, the horizontal continuity and regularity, and the proper adjacency between vertical and horizontal elements.

To complete the evaluation, the migrated depth slices acquired with the vertical configuration are presented in Fig. 11.

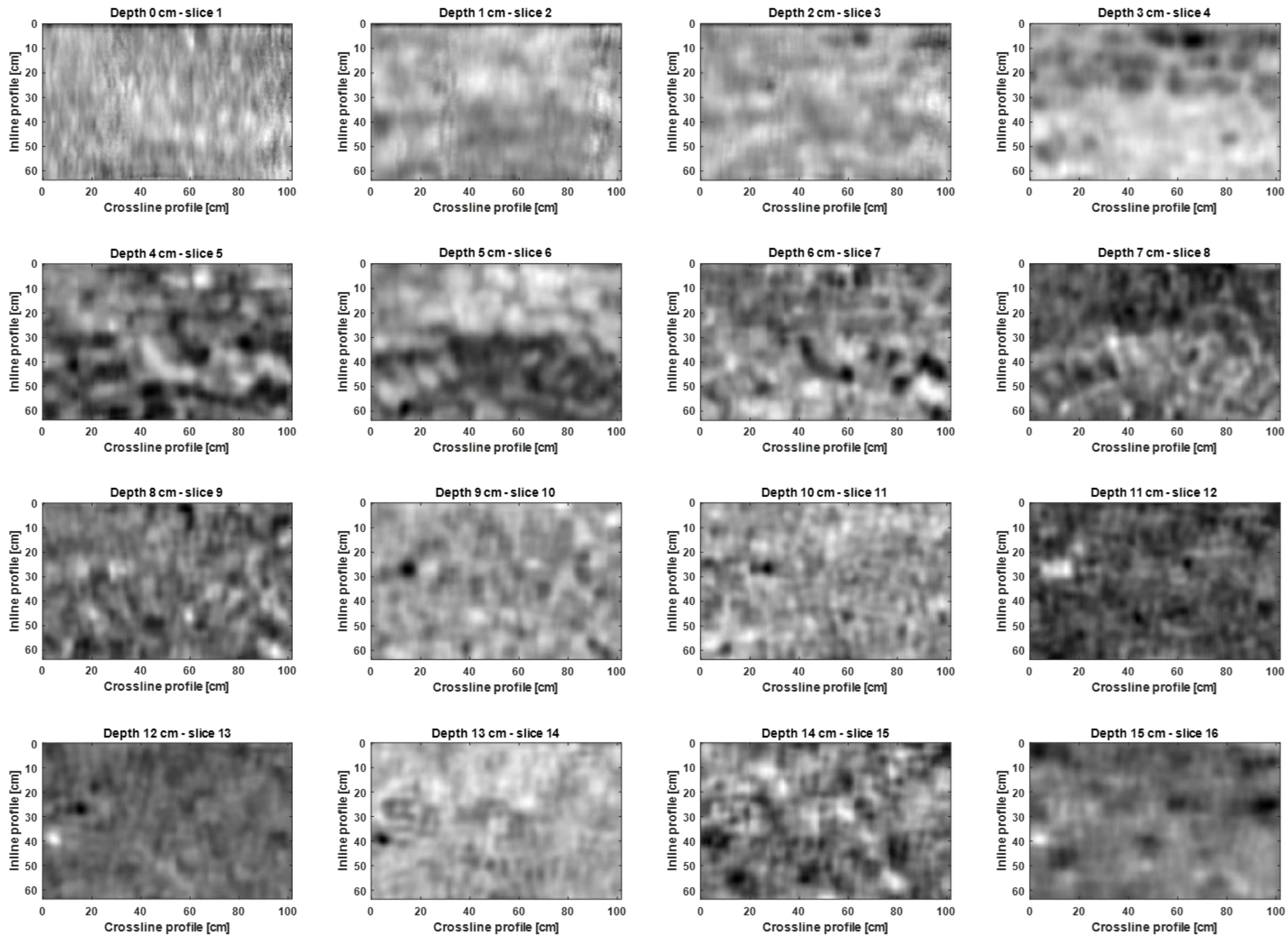

Figure 11: GPR results, migrated vertically oriented depth slices.

A very similar level of detection and reconstruction performance can be defined, following what has been commented from the analysis of Fig 9. The better delineation of vertical elements that emerged from the analysis of the unmigrated data results in a clearer definition of the brickwork core under the arch, as assessed in Fig. 12 and Table VII, respectively. The geometrical characterisation from the vertically oriented acquisition required approximately 2 to 3 slices, in agreement with the values obtained from the horizontal one.

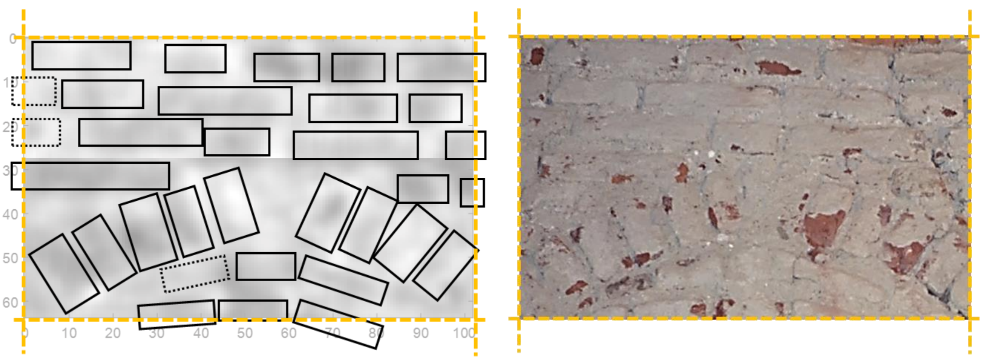

Figure 12: Reconstruction performance, migrated vertically oriented depth slices.

Table VII: Numerical reconstruction performance, migrated vertically oriented depth slices.

	Investigated area	**Investigated sector**	**Estimated number of elements**	**Actual number of elements**
	Upper area	First row	5	5
		Second row	4	5
		Third row	5	5
	Lower area	Relieving arch	9	9
		Brickwork core	8	9

Except for these evidences, the process of summing the scattering energy within the limited aperture and collapsing it at the apex of the relative diffraction have the effects of reducing the differences due to the acquisition direction, which are even less noticeable. Results of the reconstruction accuracy evaluation are provided in Table VIII.

Table VIII: Numerical reconstruction accuracy, migrated vertically oriented depth slices.

Brick example	**Element label**	**Estimated size**	**Actual size**
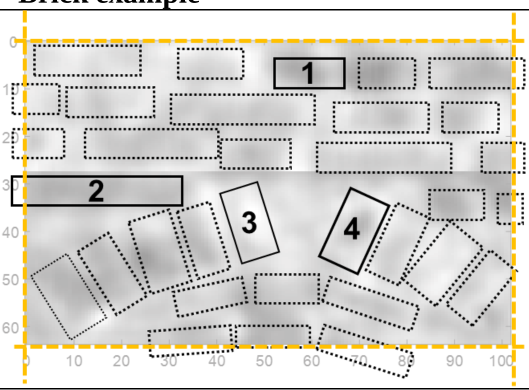	1	Height: 6 cm Length: 13 cm	Height: 6.5 cm Length: 14 cm
	2	Height: 6 cm Length: 29 cm	Height: 5 cm Length: 27 cm
	3	Height: 14 cm Length: 6 cm	Height: 12 cm Length: 6 cm
	4	Height: 11.5 cm Length: 6 cm	Height: 12 cm Length: 6.5 cm

To summarise, despite the increased processing weight required to produce the focussed results, the migration procedure has proved to be a crucial processing step to achieve a correct final interpretation, capable of providing valuable information for determining the characteristics and the morphology of a masonry wall. The analysis of the depth slices has shown that each element can be accurately located and its size estimated, all features that are involved, directly or not, in the structural assessment process.

5 – MASONRY QUALITY ESTIMATION

From the outcomes summarised in Figure 12 and Table VIII, it is possible to confidently index and label the parameters described in the introduction section, and in particular it can be stated that they are almost all fulfilled (conservation state, constituents dimension and shape, horizontal joint characteristics) or at worst, as a consequence of the remaining uncertainties, partially fulfilled (vertical joints characteristics, wall leaf connection).

This means that the surveyed area can be categorised with a high masonry quality index, and consequently a good behaviour of masonry related to both horizontal and vertical actions. Table XI describes these concepts.

Table IX: Masonry quality estimation results.

Quality parameter	Assessment	Index	GPR evidence
Conservation state of bricks and mortar and appraisable mechanical properties	Apparently in good state.	Fulfilled	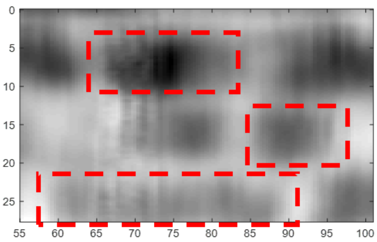
Stone/brick dimension properties	Accurately determined (examples in Table VIII). Bed: 12-14 cm Header: 6-7.5 cm Stretcher: 25-34 cm	Fulfilled	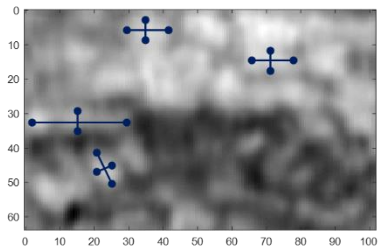
Stone/brick shape	Brickwork predominant, no evidences of stonework.	Fulfilled	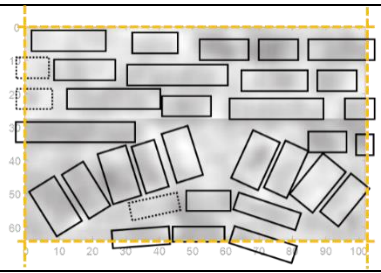

Wall leaf connections	Presence of possible headers.	Partially fulfilled	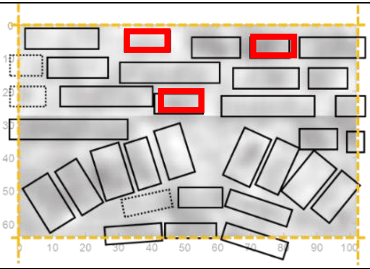
Horizontal bed joints characteristics	Continuous horizontal bed joints.	Fulfilled	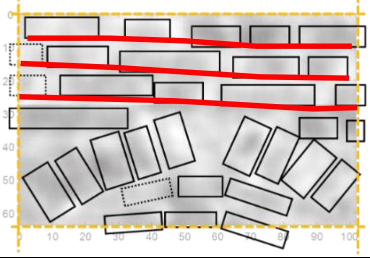
Vertical bed joint characteristics	Partially staggered vertical joints.	Partially fulfilled	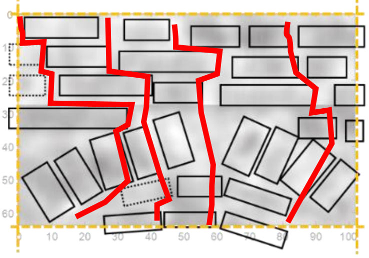

Commenting on these performances, the lower level of quality estimated for the vertical mortar lines is a result of the limited extension of such features and considering also the resolution, and hence the spatial ambiguity, achieved by the adopted GPR system. However, it can be also seen that the missing an element, in this particular case the brick under the arch, does not actually invalidate the approach, as (1) the characterisation of such parameter can still be confidently computed thanks to the obtained knowledge of the surrounding areas, and (2) the presence or absence of the brickwork has a limited impact on the masonry strength, as it is completely sustained by the overlying arch, considering also that the structural element is completely and correctly reconstructed. Regarding the headers between masonry leaves, and therefore the possibility of being in the presence of a multiple leaves masonry structure, the estimation relies in the first instance on the geometrical aspect of the brickwork, i.e. an element is defined as a candidate header based on the appearing size. Finally, the positive index on the condition state of the masonry constituents arises from the absence in the GPR slices of visible voids or significant erosion phenomena degrading the accuracy in elements delineation.

It can be therefore affirmed that the GPR survey methodology advanced in this article has demonstrated its capability in properly retrieving the majority of the required parameters needed for a quantitative masonry quality assessment, with a high level of confidence and without impacting on the wall surface at all.

Applying the methodology described in (Borri et. al. 2015a and 2015b), the investigated masonry appears to be characterised by a compressive strength (f_m) of approximately 600 N/cm^2, a shear strength (τ_0) of 9 N/cm^2, a shear modulus (G) of 640 N/cm^2 and a modulus of elasticity (E, overestimated by the methodology) of 2300 N/cm^2. Such values represent a masonry exhibiting a high carrying capacity of horizontal in- and out-of-plane actions, as well as a satisfactory resistance to the vertical ones.

As a comparison, in case the distinguishing parameters were totally fulfilling the quality requirements, the masonry strength would be enhanced of a 10 percent factor in contrasting the horizontal actions, while the shear properties would gain a 30 percent increase. Conversely, if we assume no information on the presence of headers, a decrease of the parameters defining the masonry quality can be estimated in a 16 – 20 percent range, mainly as a consequence of the contraction in the out-of-plane horizontal actions resistance. As well, the inability of adequately delineating the vertical bed joints causes an additional reduction of the parameters up to a 30 percent, or even higher (as for the shear strength value computation). In this case, such contraction is a consequence of the decreasing of the masonry resistance also to in-plane horizontal actions.

Table X details the commented performance.

Table X: Estimated masonry response comparison.

Masonry evidences	**Compression strength (f_m)**	**Shear strength (τ_0)**	**Shear modulus (G)**	**Modulus of elasticity (E)**
Ideal masonry characterisation	670 N/cm^2	13 N/cm^2	900 N/cm^2	2500 N/cm^2
From GPR survey (Table XI)	600 N/cm^2	9 N/cm^2	640 N/cm^2	2300 N/cm^2
No information on headers	480 N/cm^2	7 N/cm^2	540 N/cm^2	1950 N/cm^2
No delineation of vertical bed joints	425 N/cm^2	5.7 N/cm^2	455 N/cm^2	1780 N/cm^2

In summary, the Table once again underlines the significance of determining the presence of headers and the role of the vertical joints delineation for a proper structural assessment, features that can both be adequately addressed through a high frequency, 3D GPR investigation.

In conclusion, this study has revealed that the proposed methodology might become an operationally suitable tool to investigate a masonry structure and to provide preliminary qualitative and quantitative information on its potential behaviour to both horizontal and vertical actions. In addition, it should be considered also the well-known capability of the GPR technique of detecting wooden and metallic elements within the structure, which allows the designer to additionally understand the quality of the performed modifications or interventions and the residual resistance level.

6 – CONCLUSIONS

Within the context of the condition assessment of masonry walls for seismic behaviour characterisation, and generally for structure inspection and diagnosis, this study has demonstrated the successful application of GPR technique in retrieving essential information on the masonry typology and the geometrical properties of its constituent elements (brick, stone and mortar) properties, a knowledge that is typically achieved through the use of more invasive approach and consequently with a limited scalability. In particular, the aim was to evaluate the performance of the methodology in determining the presence, the partial presence, or the absence of specific construction features that could provide a quantitative indication of the quality of the masonry.

Therefore, the challenges addressed are associated not only with the detection of shallow targets with limited size and potentially a similar dielectric behaviour, but also with their precise reconstruction, accurately enough to allow for the extraction of the masonry quality parameters, a set of attributes which includes among others the delineation of the mortar joint and the constituent elements dimensions. These scopes have required the deployment of a dedicated 3D, high frequency GPR platform.

Results have been obtained for both unmigrated and focussed GPR slices, as well as acquired along different survey directions, and their analysis has highlighted that unmigrated data only provide a qualitative characterisation of the surveyed area, adequate for determining typology and texture morphology, but the achieved performance in terms of single element reconstruction are limited. On the contrary, the migration algorithm has the effect of improving the readability of the produced images, thus consequently reducing the influence of the user confidence in interpreting the data, and allows for an encouraging recognition and geometrical reconstruction of all the elements composing the masonry, retrieving almost the entire set of parameters needed for the masonry quality assessment.

Research remains to exploit some important aspects, first of all a clearer and improved identification of the number of headers, considering its importance in determining the wall capacity to resist seismic actions (as highlighted in Table X). This can be done by acquiring a correspondent area on the other side of the wall, considering that a properly connected multi-leaf connection requires elements traversing the entire wall structure, and hence location matches between potential header candidates can expectedly identify the fulfilment of such structural property. Another aspect requiring attention for a deeper seismic behaviour characterisation is the identification of toothing, i.e. the process of constructing the temporary end of a wall with the end stretcher of every alternate course projecting, at the wall-to-tie-column interface, either being at an interior or at corner, as well as toothing at cross walls intersections. Such confinement technique ensures a satisfactory bond between adjacent structural elements, controlling the out-of-plane behaviour and therefore improving the building robustness and ductility against seismic forces.

From an engineering perspective, future works will be focussed on the automation of the detection, recognition and identification process through the development of dedicated image processing algorithms, so that the reliance upon the user interpretation ability can be further reduced and the system performance improved. Another advancement that can be put forward is the conceptualisation of a flexible, wide-scale survey equipment for an efficient and productive application on site, seamlessly integrating the sensor and the positioning equipment.

Acknowledgements

This work was supported by Regione Lombardia through the Non Tremare project (grant ID 379246) under the Smart Living programme.

References

[1] Borri A., Corradi M., Castori G. and De Maria A. (2015). A method for the analysis and classification of historic masonry. Bulletin of Earthquake Engineering, 13, 2647-2665. doi: 10.1007/s10518-015-9731-4

[2] Borri A., Castori G., and Corradi M. (2015). Determination of Shear Strength of Masonry Panels Through Different Tests. International Journal of Architectural Heritage. 9(8), 913- 927. doi: 10.1080/15583058.2013.804607

[3] Lagomarsino S., and Podestà S. (2004) Seismic vulnerability of ancient churches: II. Statistical analysis of surveyed data and methods for risk analysis. Earthquake Spectra, 20(2), 395–412. doi: 10.1193/1.1737736

[4] Lourenço P.B., Mendesa N., Ramosa L.F., Oliveira D.V. (2011) Analysis of masonry structures without box behavior. International Journal of Architectural Heritage, 5 (4–5), 369–382. doi: 10.1080/15583058.2010.528824

[5] Zuccaro, G., Cacace, F. (2015) Seismic vulnerability assessment based on typological characteristics. The first level procedure "SAVE", Soil Dynamics and Earthquake Engineering, 69, 262-269. doi: 10.1016/j.soildyn.2014.11.003

[6] Taffarel, S., Caliman, M., Valluzzi, M.R., Modena, C. (2016). Seismic vulnerability assessment of clustered historical centers: Fragility curves based on local collapse mechanisms analyses. In 16th International Brick and Block Masonry Conference, Trends, Innovations and Challenges, Padua, Italy, June 2016; 2463 – 2470. doi: 10.1201/b21889-322

[7] Perelli, F.L.de Gregorio, D.,Cacace, F. and Zuccaro, G. (2019) Empirical vulnerability curves for Italian masonry buildings, In 7th International Conference on Computational Methods in Structural Dynamics and Earthquake Engineering, Crete; Greece; June 2019, 1745-1758, doi: 10.7712/120119.7033.19864

[8] Borri, A., De Maria, A., Casaglia S. (2014). The EAL-M method for the seismic classification of the existing masonry buildings: a comparison between different methods and preliminary evaluations of other typologies. (in Italian) Progettazione Sismica, 5(2), 11-29, 10.7414/PS.5.2.11-29.

[9] Erberik, A.M. (2008) Generation of fragility curves for Turkish masonry buildings considering in-plane failure modes. Earthquake Engineering Structural Dynamics, 37(3): 387–405. 10.1002/eqe.760.

[10] Rota M., Penna, A., Magenes G. (2010). A methodology for deriving analytical fragility curves for masonry buildings based on stochastic nonlinear analyses. Engineering Structures, 32(5), 1312-1323, 10.1016/j.engstruct.2010.01.009.

[11] Pagnini, L.C., Vicente, R., Lagomarsino, S., Varum, H. (2011). A mechanical model for the seismic vulnerability assessment of old masonry buildings. Earthquakes and Structures, 2(1), 25-42. 10.12989/eas.2011.2.1.025

[12] Garavaglia E., Anzani A., Maroldi F., Vanerio F. (2020) Non-Invasive Identification of Vulnerability Elements in Existing Buldings and Their Visualization in the BIM Model for Better Project Management: The Case Study of Cuccagna Farmhouse. Applied Sciences, 10(6), 2119, 10.3390/app10062119

[13] Benedetto, A., Pajewski, L. (Eds.). (2015). Civil engineering applications of ground penetrating radar. Springer. doi: 10.1007/978-3-319-04813-0

[14] Daniels, D.J. Ground Penetrating Radar, 2nd ed.; The Institution of Electrical Engineers: London, UK, 2004; 565 doi: 10.1002/0471654507.eme152

[15] Barraca, N., Almeida, M., Varum, H., & Matias, M. S. (2014). The use of GPR in the rehabilitation of built heritage. In Near Surface Geoscience 2014-20th European Meeting of Environmental and Engineering Geophysics, Athens, Greece, September 2014, 1-5. doi: 10.3997/2214-4609.20141998.

[16] De Donno, G., Di Giambattista, L., & Orlando, L. (2017). High-resolution investigation of masonry samples through GPR and electrical resistivity tomography. Construction and Building Materials, 154, 1234-1249. doi: 10.1016/j.conbuildmat.2017.06.112

[17] Lai, W. W. L., Derobert, X., & Annan, P. (2018). A review of Ground Penetrating Radar application in civil engineering: A 30-year journey from Locating and Testing to Imaging and Diagnosis. NDT & E International, 96, 58-78. doi: 10.1016/j.ndteint.2017.04.002

[18] Martini, R., Carvalho, J., Barraca, N., Arêde, A., & Varum, H. (2017). Advances on the use of non-destructive techniques for mechanical characterization of stone masonry: GPR and sonic tests. Procedia Structural Integrity, 5, 1108-1115. doi: 10.1016/j.prostr.2017.07.096.

[19] McCann, D. M., & Forde, M. C. (2001). Review of NDT methods in the assessment of concrete and masonry structures. Ndt & E International, 34(2), 71-84. doi: 10.1016/S0963-8695(00)00032-3.

[20] Angiulli, G., Barrile, V., Cacciola, M. The GPR technology on the seisimic damageability assessment of reinforced concrete building. In 2005 Progress in Electromagnetics Research Symposium, Hangzhou, China, August 2005, 1(3), 303-307. doi: 978-193307707-9

[21] Diamanti, N., Giannopoulos, A., & Forde, M. C. (2008). Numerical modelling and experimental verification of GPR to investigate ring separation in brick masonry arch bridges. NDT & E International, 41(5), 354-363. doi: 10.1016/j.ndteint.2008.01.006

[22] Solla, M., Lorenzo, H., Rial, F. I., Novo, A. (2012). Ground-penetrating radar for the structural evaluation of masonry bridges: Results and interpretational tools. Construction and Building Materials, 29, 458-465. doi: 10.1016/j.conbuildmat.2011.10.001

[23] Tosti, F., Ferrante, C. Using Ground Penetrating Radar Methods to Investigate Reinforced Concrete Structures. Surv Geophys 41, 485–530 (2020). doi: 10.1007/s10712-019-09565-5

[24] Barrile, V., & Pucinotti, R. (2005). Application of radar technology to reinforced concrete structures: a case study. NDT & E International, 38(7), 596-604. doi: 10.1016/j.ndteint.2005.02.003

[25] Binda, L., Zanzi, L., Lualdi, M., & Condoleo, P. (2005). The use of georadar to assess damage to a masonry Bell Tower in Cremona, Italy. NDT & E International, 38(3), 171-179. doi: 10.1016/j.ndteint.2004.03.010

[26] Catapano, I.; Ludeno, G.; Soldovieri, F.; Tosti, F.; Padeletti, G. Structural Assessment via Ground Penetrating Radar at the Consoli Palace of Gubbio (Italy). Remote Sensing, 10(1), 45. doi: 10.3390/rs10010045.

[27] Perez-Gracia, V., Santos-Assuncao, S., Caselles, O., Clapés, J., & Canas, J. A. (2014). Study of wood beams in buildings with ground penetrating radar. In 15th International Conference on Ground Penetrating Radar, June 2014, Brussels, Belgium, 31-35. doi: 10.1109/ICGPR.2014.6970379.

[28] Santos-Assunçao, S., Perez-Gracia, V., Caselles, O., Clapes, J., & Salinas, V. (2014). Assessment of complex masonry structures with GPR compared to other non-destructive testing studies. Remote Sensing, 6(9), 8220-8237. doi: 10.3390/rs6098220

[29] Binda L., Saisi A. and Tiraboschi C. (2000). Investigation procedures for the diagnosis of historic masonries. Construction and Building Material, 14, 199–233. doi: 10.1016/S0950-0618(00)00018-0

[30] Borri, A., De Maria, (2015). Masonry Quality Index (MQI): correlation with the mechanical characteristics and knowledge levels (in Italian). Progettazione Sismica, 6(3), 45-63, 10.7414/PS.6.3.45-63.

[31] Colla, C., Fernàndez, A. J., Garanzini, S., & Marelli, M. (2010). Diagnostic by imaging: 3D GPR investigation of brick masonry and post-tensioned concrete. In 13th International Conference on Ground Penetrating Radar, Lecce, Italy, August 2012, 1-7. doi: 10.1109/ICGPR.2010.5550175

[32] Hamrouche, R., Klysz, G., Balayssac, J. P., Rhazi, J., Ballivy, G. (2012). Numerical simulations and laboratory tests to explore the potential of Ground-Penetrating Radar (GPR) in detecting unfilled joints in brick masonry structures. International Journal of Architectural Heritage, 6(6), 648-664. doi: 10.1080/15583058.2011.597484

[33] Pérez-Gracia, V., Solla, M. (2015). Inspection procedures for effective GPR surveying of buildings. In Civil Engineering Applications of Ground Penetrating Radar, Springer, Cham. 97-123, doi: 10.1007/978-3-319-04813-0_4

[34] Negri, S., & Aiello, M. A. (2020). High-resolution GPR survey for masonry wall diagnostics. Journal of Building Engineering, 33, 1-11, doi: 101817. 10.1016/j.jobe.2020.101817

[35] Lombardi, F., Griffiths, H. D., Lualdi, M., & Balleri, A. (2020). Characterization of the Internal Structure of Landmines Using Ground-Penetrating Radar. IEEE Geoscience and Remote Sensing Letters. Early Access, doi: 10.1109/LGRS.2020.2970249

[36] Luo, T. X., Lai, W. W., Chang, R. K., & Goodman, D. (2019). GPR imaging criteria. Journal of Applied Geophysics, 165, 37-48. doi: 10.1016/j.jappgeo.2019.04.008

[37] Pieraccini, M., Miccinesi, L. (2018). No-contact GPR for investigating painted walls. In 2018 17th International Conference on Ground Penetrating Radar, Rapperswil, Switzerland, June 2018, 1-6. doi: 10.1109/ICGPR.2018.8441580

[38] Pomfret, J. (2006). Ground- penetrating radar profile spacing and orientation for subsurface resolution of linear features. Archaeological Prospection, 13(2), 151-153. doi: 10.1002/arp.285

[39] Samet, R., Çelik, E., Tural, S., Şengönül, E., Özkan, M., & Damcı, E. (2017). Using interpolation techniques to determine the optimal profile interval in ground-penetrating radar applications. Journal of Applied Geophysics, 140, 154-167. doi: 10.1016/j.jappgeo.2017.04.003

[40] Lombardi, F., Griffiths, H. D., & Lualdi, M. (2018). Sparse Ground Penetrating Radar Acquisition: Implication for Buried Landmine Localization and Reconstruction. IEEE Geoscience and Remote Sensing Letters, 16(3), 362-366. doi: 10.1109/LGRS.2018.2872357

[41] Lualdi, M. (2011). "True" 3D Acquisition using GPR Over Small Areas: A Cost Effective Solution. In 24rd EEGS Symposium on the Application of Geophysics to Engineering and Environmental Problems, Charleston, USA, April 2011, 541-550. doi: 10.3997/2214-4609-pdb.247.21

[42] Pieraccini, M., Pisaneschi, M., Noferini, L., & Atzeni, C. (2007). Polarimetric radar signature of masonry walls. NDT & E International, 40(4), 271-274. doi: 10.1016/j.ndteint.2006.11.004.

[43] Lualdi, M., Lombardi, F. (2014). Significance of GPR polarisation for improving target detection and characterisation, Nondestructive Testing and Evaluation, 29 (4), 345-356. doi: 10.1080/10589759.2014.949708